AMERICAN SOCIETY FOR MICROBIOLOGY | Applied and Environmental Microbiology®

GEOMICROBIOLOGY

Lack of Methylated Hopanoids Renders the Cyanobacterium *Nostoc punctiforme* Sensitive to Osmotic and pH Stress

Tamsyn J. Garby,[a] Emily D. Matys,[b] Sarah E. Ongley,[a,c] Anya Salih,[d] Anthony W. D. Larkum,[e] Malcolm R. Walter,[a] Roger E. Summons,[b] Brett A. Neilan[a,c]

Australian Centre for Astrobiology and School of Biotechnology and Biomolecular Sciences, The University of New South Wales, Sydney, NSW, Australia[a]; Department of Earth, Atmospheric and Planetary Sciences, Massachusetts Institute of Technology, Cambridge, Massachusetts, USA[b]; School of Environmental and Life Sciences, The University of Newcastle, Callaghan, NSW, Australia[c]; Confocal Bioimaging Facility, Western Sydney University, Penrith, NSW, Australia[d]; Plant Functional Biology and Climate Change Cluster, University of Technology Sydney, NSW, Australia[e]

ABSTRACT To investigate the function of 2-methylhopanoids in modern cyanobacteria, the *hpnP* gene coding for the radical *S*-adenosyl methionine (SAM) methylase protein that acts on the C-2 position of hopanoids was deleted from the filamentous cyanobacterium *Nostoc punctiforme* ATCC 29133S. The resulting Δ*hpnP* mutant lacked all 2-methylhopanoids but was found to produce much higher levels of two bacteriohopanepentol isomers than the wild type. Growth rates of the Δ*hpnP* mutant cultures were not significantly different from those of the wild type under standard growth conditions. Akinete formation was also not impeded by the absence of 2-methylhopanoids. The relative abundances of the different hopanoid structures in akinete-dominated cultures of the wild-type and Δ*hpnP* mutant strains were similar to those of vegetative cell-dominated cultures. However, the Δ*hpnP* mutant was found to have decreased growth rates under both pH and osmotic stress, confirming a role for 2-methylhopanoids in stress tolerance. Evidence of elevated photosystem II yield and NAD(P)H-dependent oxidoreductase activity in the Δ*hpnP* mutant under stress conditions, compared to the wild type, suggested that the absence of 2-methylhopanoids increases cellular metabolic rates under stress conditions.

IMPORTANCE As the first group of organisms to develop oxygenic photosynthesis, *Cyanobacteria* are central to the evolutionary history of life on Earth and the subsequent oxygenation of the atmosphere. To investigate the origin of cyanobacteria and the emergence of oxygenic photosynthesis, geobiologists use biomarkers, the remnants of lipids produced by different organisms that are found in geologic sediments. 2-Methylhopanes have been considered indicative of cyanobacteria in some environmental settings, with the parent lipids 2-methylhopanoids being present in many contemporary cyanobacteria. We have created a *Nostoc punctiforme* Δ*hpnP* mutant strain that does not produce 2-methylhopanoids to assess the influence of 2-methylhopanoids on stress tolerance. Increased metabolic activity in the mutant under stress indicates compensatory alterations in metabolism in the absence of 2-methylhopanoids.

KEYWORDS BHP, BHT, *Nostoc punctiforme*, cyanobacteria, hopanoid

Received 18 April 2017 **Accepted** 26 April 2017

Accepted manuscript posted online 28 April 2017

Citation Garby TJ, Matys ED, Ongley SE, Salih A, Larkum AWD, Walter MR, Summons RE, Neilan BA. 2017. Lack of methylated hopanoids renders the cyanobacterium *Nostoc punctiforme* sensitive to osmotic and pH stress. Appl Environ Microbiol 83:e00777-17. https://doi.org/10.1128/AEM.00777-17.

Editor Frank E. Löffler, University of Tennessee and Oak Ridge National Laboratory

Copyright © 2017 American Society for Microbiology. All Rights Reserved.

Address correspondence to Roger E. Summons, rsummons@mit.edu, or Brett A. Neilan, brett.neilan@newcastle.edu.au.

Bacteriohopanepolyols (BHPs) are pentacyclic triterpenoids hypothesized to be functional analogs of eukaryotic sterols, and they are widely used as biomarkers for bacteria (1). Hopane hydrocarbons, the diagenetic products of BHPs, are ubiquitous and abundant in ancient sediments (2); therefore, they are potentially useful for evaluating

Downloaded from http://aem.asm.org/ on June 7, 2018 by guest

past microbial communities and paleoenvironmental conditions. To this end, it is important to increase our understanding of the sources and functions of specific hopanoid structures. Knowledge about how bacteria adjust their hopanoid production to adapt to different conditions enhances the diagnostic value of fossil lipid assemblages in geologic samples.

Hopanoids occur in a wide range of Gram-negative and Gram-positive bacteria, including those that form symbiotic associations with plants (3, 4); yet, large gaps still exist in our understanding of the breadth of the physiological functions of hopanoids. The localization of hopanoids in membranes has been documented in a variety of different bacteria (5–8). It appears that these lipids influence outer membrane order and integrity by interacting with lipid A in a manner analogous to that of cholesterol with sphingolipids in eukaryotes (9–13). There is mounting evidence for the role of hopanoids in protecting cells against a variety of stress conditions, such as increased temperature (5, 14–18), pH and osmotic tension (16, 18, 19), and desiccation (20).

Due to their structural stability, 2-methylhopanoids (2-MeBHPs) in particular are of significant geobiological interest. 2-MeBHPs have been found in significant quantities in both cyanobacterial cultures and cyanobacterium-dominated microbial mats (21, 22), with over 20 strains of cyanobacteria across multiple orders testing positive for 2-MeBHP (reviewed in reference 23). Furthermore, episodic spikes in 2-MeBHP abundances in ancient marine sediments and derived oils have been interpreted as possible indicators of modern cyanobacteria thriving during oceanic anoxic events (24, 25). However, a complicating factor is that, despite their distribution across all orders of *Cyanobacteria*, not all or even a majority of cyanobacteria have the capability to produce 2-MeBHPs (23; T. J. Garby and B. A. Neilan, unpublished data).

2-MeBHPs have also long been known to be produced by bacteria other than cyanobacteria (26–30). It was initially thought that these taxa produced only small amounts of 2-MeBHP, which could not account for the abundance of 2-MeBHP in sediments and petroleum. However, it has recently been shown that the anoxygenic phototroph *Rhodopseudomonas palustris* produces 2-MeBHPs in significant amounts (31). In addition to this, phylogenetic analysis of HpnP, responsible for the C-2 methylation of BHPs to produce 2-MeBHP, showed a wide distribution in *Alphaproteobacteria*; this also suggested that it was unlikely that *hpnP* originated in *Cyanobacteria* (32). This brought into question the validity of using 2-methylhopanes as taxonomic biomarkers for cyanobacteria and led to the proposal that 2-MeBHPs may instead be more generally diagnostic for specific ecological niches (33).

In light of these uncertainties, it is important to learn more about the distribution and physiological role(s) of 2-MeBHPs in cyanobacteria and other bacteria where they are present. Apart from acting as membrane rigidifiers (10), which in turn can influence membrane protein function and transport, the specific functions of 2-MeBHPs in modern cyanobacteria are not well understood. However, it has been shown that 2-MeBHPs are most abundant in the outer membranes of certain cell types, suggesting that C-2 methylation may promote stress resistance (34).

Hopanoids are produced by *N. punctiforme* ATCC 29133 (PCC 73102), a filamentous cyanobacterium of the order *Nostocales*. This cyanobacterium was originally isolated from a root section taken from a *Macrozamia* sp. cycad (35) and can form symbiotic associations with a number of different plant genera (36). The relationship between *N. punctiforme* and its environment is particularly interesting, as this species can differentiate into a number of cell types in response to external factors (37). Photosynthetic vegetative cells are the usual cell type under normal conditions, but several specialized cell types can form under stressful conditions. The absence of a nitrogen source leads to the formation of specialized nonphotosynthetic heterocysts capable of fixing atmospheric nitrogen (N_2). Additionally, resting cells called akinetes form in response to nutrient or light limitation. Akinetes are larger and more resistant to stress than vegetative cells, allowing survival until conditions are favorable for growth. Last, hormogonia, gliding filaments that are much more motile than vegetative filaments

Downloaded from http://aem.asm.org/ on June 7, 2018 by guest

and composed of smaller cells, form in response to a variety of environmental stress signals.

The complex life cycle of *N. punctiforme* makes it particularly suited for studying the role of hopanoids in stress acclimation. Different cell types contain altered hopanoid profiles, with 2-MeBHP levels being greatest in the outer membranes of akinetes and vegetative cells in N_2-fixing cultures (34). The genome of *N. punctiforme* ATCC 29133 has been sequenced (38), allowing for the identification of genes known to be required for BHP biosynthesis, and particularly that for 2-MeBHP (39). Bacteriohopanetetrol and two isomers of bacteriohopanepentol, bacteriohopane-31,32,33,34,35-pentol (BHpentol-1) and bacteriohopane-30,32,33,34,35-pentol isomer (BHpentol-2), along with their 2-methylated counterparts, have previously been detected in *Nostoc muscorum*, *Nostoc* sp. strain PCC 6720, and *Nostoc* sp. strain ATCC 27985 (26, 40, 41). BHpentol-2, bearing a hydroxyl group on C-30, has not been reported in taxa other than *Nostoc* spp. and this, together with the R configuration of the hydroxyl at C-34, may be unique to this genus (41).

In this study, we sought to evaluate proposed links between 2-MeBHP and environmental stress (33, 42), based on geological evidence that suggests some sediments contain anomalously high levels of 2-methylhopanes, implicating them as being important for microbial survival (43–45). Specifically, we investigated the role of 2-MeBHPs in a modern cyanobacterium conferring adaptations to various environmental conditions. To this end, the gene coding for the hopanoid C-2 methylase, *hpnP* (39), was inactivated in *Nostoc punctiforme* ATCC 29133S (46). As 2-MeBHPs have previously been linked to roles in both and stress tolerance and akinete formation, it was expected that the absence of 2-methylhopanoid would adversely affect cell survival under a variety of stress conditions and negatively impact the production of akinetes.

RESULTS

Confirmation of gene inactivation. PCR amplification and sequencing of *hpnP* and flanking loci showed the successful replacement of the central region of the *hpnP* gene with the neomycin resistance cassette of plasmid pSCR9. Additionally, PCRs performed with primers internal to the deleted section of the *hpnP* gene failed to amplify any product from the genomes of mutated cells.

Hopanoid profiles. Hopanoid analyses of *N. punctiforme* wild-type and Δ*hpnP* mutant vegetative and akinete cells revealed six BHP compounds (Fig. 1). Bacteriohopanetetrol (BHtetrol) and its methylated counterpart, 2-methylbacteriohopanetetrol (2-MeBHtetrol), were present in wild-type vegetative and akinete cell types. BHtetrol was present, while 2-MeBHtetrol was absent, in all Δ*hpnP* mutants. Bacteriohopanepentol (BHpentol) was identified, as well as putative isomers denoted BHpentol-1 and BHpentol-2. 2-Methylbacteriohopanepentol (2-MeBHpentol) was also identified, as well as putative isomers denoted 2-MeBHpentol-1 and 2-MeBHpentol-2. 2-MeBHpentol-1 and 2-MeBHpentol-2 were the most abundant compounds in wild-type vegetative and akinete cell types and were absent in all Δ*hpnP* mutant cell types. BHpentol-2 and 2-MeBHpentol-2 were not detected by gas chromatography-mass spectrometry (GC-MS) and required liquid chromatography-MS (LC-MS) techniques for identification.

A clear change was observed in the diversity and abundance of BHPs produced by wild-type *N. punctiforme* and Δ*hpnP* mutant strain cell types (Fig. 2). LC-MS analysis using authentic standards enabled the robust quantification of BHP compounds (Fig. 1). Total BHP is greater in vegetative cells than in the akinete cell type in both wild type and Δ*hpnP* mutants. Total BHP is greater in wild-type cells (vegetative and akinete) than in Δ*hpnP* mutant cells. While Δ*hpnP* vegetative and akinete cell mutants do not produce 2-MeBHP, the abundances of BHpentol-1, BHpentol-2, and BHtetrol increase, possibly compensating for the lack of 2-MeBHPs produced. Both wild-type vegetative and akinete cells contained an order of magnitude more methylated BHPs than desmethyl BHPs. Total BHP is ~75% greater in wild-type vegetative cells than in wild-type akinetes. However, total BHP is only ~35% greater in Δ*hpnP* mutant vegetative cells than in Δ*hpnP* mutant akinetes. Wild-type cells still produce ~30% more BHPs than Δ*hpnP* mutants due to their high abundance of nonmethylated compounds.

Downloaded from http://aem.asm.org/ on June 7, 2018 by guest

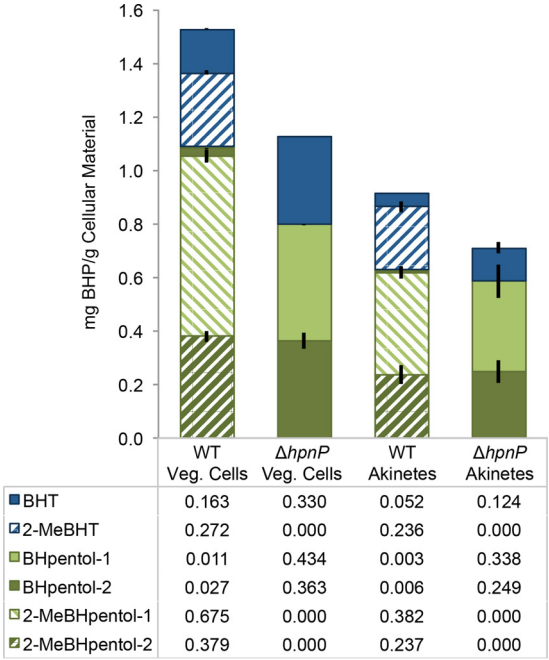

FIG 1 Abundance of hopanoids as analyzed by LC-MS. The lipid content of wild-type (WT) and Δ*hpnP* mutant cultures dominated by late-exponential-phase vegetative (Veg.) cells or akinetes was characterized. Hopanoids (milligrams of BHPs per gram of lyophilized cellular material) detected in each sample are given below the cellular type. Quantification was completed using authentic BHtetrol and 2-MeBHtetrol standards. Values were averaged from 2 LC-MS runs (4 June 2014 and 16 June 2015). Error bars represent 1 standard deviation.

Akinete formation. Cultures were induced to form akinetes to determine if the lack of 2-methylhopanoids impeded this process. Akinete formation was not affected by the lack of 2-methylhopanoids, with the Δ*hpnP* mutant culture forming filaments of akinetes as readily as the wild-type culture (Fig. 3 and 4). Confocal imaging revealed no differences in the cell shape, size, or fluorescence emission intensity between wild-type and Δ*hpnP* mutant *N. punctiforme*. Akinete-dominated cultures had more-rounded cells, and many were larger in size than the vegetative cells (Fig. 4A and B). It was also observed that hormogonium filaments formed alongside the akinetes in the wild-type culture, whereas in the Δ*hpnP* mutant culture, hormogonium filaments were rare.

Fluorescence emissions were highest in the orange and the red wavebands due to phycobilins and chlorophyll (Fig. 4). Microspectral confocal imaging identified prominent *in vivo* emission peaks due to the photosynthetic pigments typical of *Nostoc* species. These were due to phycoerythrin (PE), with an emission maximum (em_{max}) at 575 nm; phycocyanin (PC), with an em_{max} of 625 to 645 nm; allophycocyanin (ALP), with an em_{max} of 660 to 665 nm; shoulders at 675 to 690 nm (chlorophyll *a* photosystem II [chl PSII]); and far-red emissions at 710 nm (chl photosystem I [chl PSI]) (Fig. 4C).

There was a distinct increase in the PE emissions relative to other peaks in akinetes, which was most prominent in Δ*hpnP* mutant cells and lowest in the Δ*hpnP* mutant vegetative cells (Fig. 4C). Akinetes were also observed to have reduced levels of ALP, as well as chl *a* PSII and PSI emissions, compared to the vegetative cells (Fig. 4C). The differences were especially prominent in Δ*hpnP* mutant cells. Since 2-methylhopanoids are not known to be functionally linked to oxygenic photosynthesis, the cause of these differences in pigment expression in Δ*hpnP* mutant cells is presently unknown.

Mutant response to temperature stress. *N. punctiforme* ATCC 29133S wild-type and Δ*hpnP* mutant cultures were subjected to stress caused by elevated temperature and freezing/thawing. Based on chl *a* levels, cultures of *N. punctiforme* Δ*hpnP* mutant cells grown at 34°C did not grow significantly more slowly than wild-type cultures (Fig. 5). Cultures of *N. punctiforme* Δ*hpnP* mutant cells frozen and thawed over a period of

Downloaded from http://aem.asm.org/ on June 7, 2018 by guest

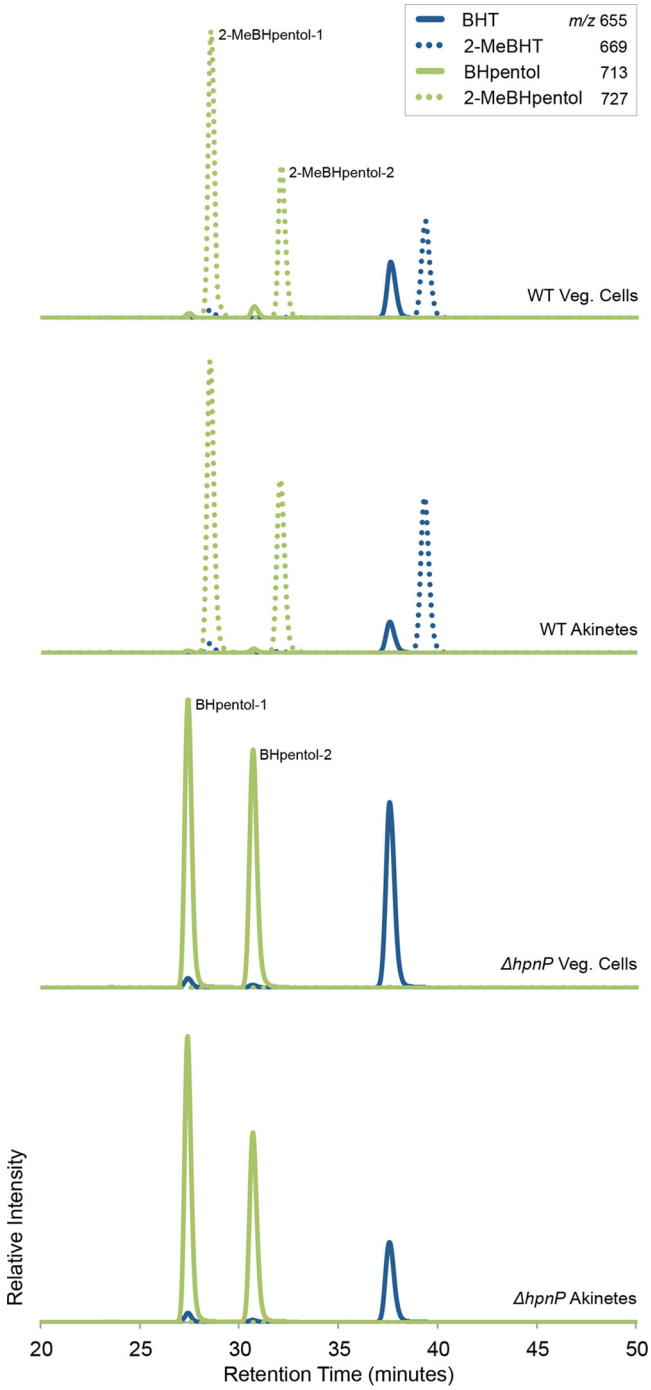

FIG 2 Typical LC chromatograms showing the elution patterns of acetylated hopanoids from wild-type (WT) and Δ*hpnP* mutant cultures dominated by vegetative cells or akinetes. BHpentol-1 is tentatively identified as bacteriohopane-31,32,33,34,35-pentol based on its elution position relative to that compound in other samples. BHpentol-2 is assigned as bacteriohopane-30,32,33,34,35-pentol, previously identified by Zhao et al. (41). The 2-methyl analogs of these compounds are identified, similarly, by their relative retention times. BHT is bacteriohopane-32,33,34,35-tetrol and 2-MeBHT is its 2-methyl analog.

2 weeks and then used to inoculate media and incubated at 25°C failed to grow in two out of three replicates, as opposed to cultures from similarly treated *N. punctiforme* wild-type cultures, where all three replicates recovered and resumed growth. The maximum quantum yield of the photosystem (F_v/F_m; see Materials and Methods) was measured for control cultures and heat-treated cultures over the course of 5 weeks to

Downloaded from http://aem.asm.org/ on June 7, 2018 by guest

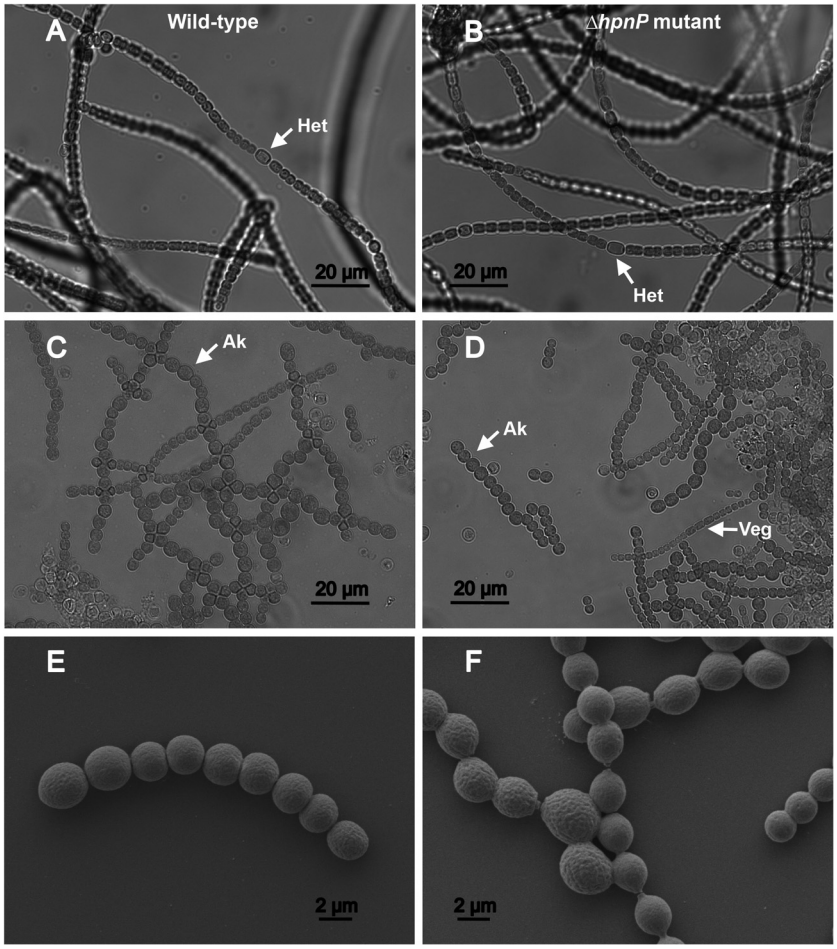

FIG 3 Differential interference contrast micrographs (A to D) and scanning electron microscopy (SEM) images (E and F) of cultures of wild-type *N. punctiforme* (A, C, and E) and the Δ*hpnP* mutant (B, D, and F), under control conditions (A and B) showing vegetative cell filaments with heterocysts (Het), and 16 weeks after transfer to phosphate-free medium and low light conditions (C to F), showing formation of akinetes (Ak) among vegetative filaments (Veg).

obtain a measurement of photosynthetic efficiency as an indication of cell health (see Fig. S3A in the supplemental material). F_v/F_m values for both heat-stressed cultures were consistently higher than the F_v/F_m values for both control condition cultures. There was no significant difference in F_v/F_m values between *N. punctiforme* wild-type and Δ*hpnP* mutant cells under either control or heat stress conditions.

Mutant response to variable pH. *N. punctiforme* ATCC 29133 wild-type and Δ*hpnP* mutant cultures were subjected to different pH values in two separate experimental designs. At pH 9.5, the growth rates of both the wild-type and Δ*hpnP* mutant did not significantly vary from that under the control conditions (Fig. 5). The growth rates for both treated cultures began to decline after 10 days; however, the wild type did not vary considerably from the control over the course of the experiment, indicating a faster stress adaptation. The culture density of the Δ*hpnP* mutant was significantly lower than that of the wild type after 23 days, supporting a faster adaptation of the wild type to the high-pH-stress condition.

When a range of pH values were tested over several weeks, there was a significant difference in culture density between the wild-type and Δ*hpnP* mutant strains grown at pH levels of 6.0, 6.2, 6.5, 6.8, and 7.0 after 5 weeks (Fig. 6A). Cultures grown at higher pH values (7.8 to 9.0) did not survive the duration of the experiment.

F_v/F_m was measured for control cultures and cultures grown at pH 6.0 and pH 9.5 over the course of 5 weeks (Fig. S3B). F_v/F_m values for cultures grown at pH 6.0 were

Downloaded from http://aem.asm.org/ on June 7, 2018 by guest

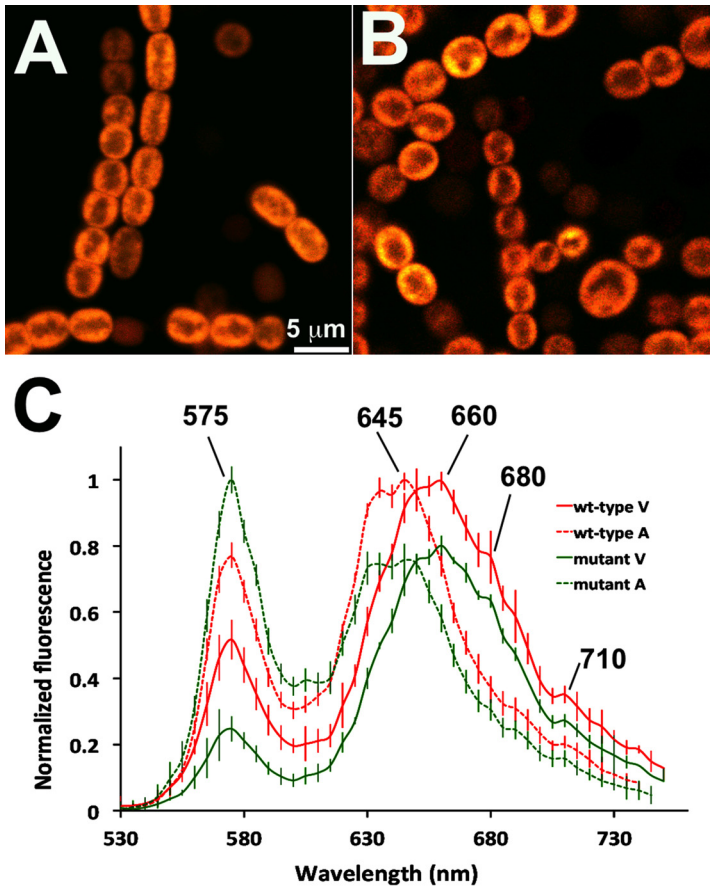

FIG 4 Confocal imaging of fluorescence emissions of *N. punctiforme* with emissions from PMT 1 (520 to 620 nm) and PMT 2 (638 to 700 nm) combined. (A) Akinete-dominated culture of the wild type. (B) Δ*hpnP* mutant stages. (C) Confocal microspectral detection of photosynthetic pigments in wild-type vegetative stages (red solid line) and akinete stages (red dashed line) and the Δ*hpnP* mutant vegetative (green solid line) and mutant akinete (dashed green line) stages. The spectral emission peaks are at: 575 nm for phycoerythrin (PE), 645 nm for phycocyanin (PC), 660 nm for allophycocyanin (APC), the shoulder at 680 nm for chlorophyll *a* photosystem II (chl PSII), and 710 nm for chl photosystem I (Chl PSI).

no different from those grown under control conditions, and there was also no difference between the F_v/F_m values of wild-type and Δ*hpnP* mutant cultures. The F_v/F_m values for cultures grown at pH 9.5 varied over time, with a drop in F_v/F_m around days 13 to 30 corresponding to a decreased growth rate over this period. The F_v/F_m values

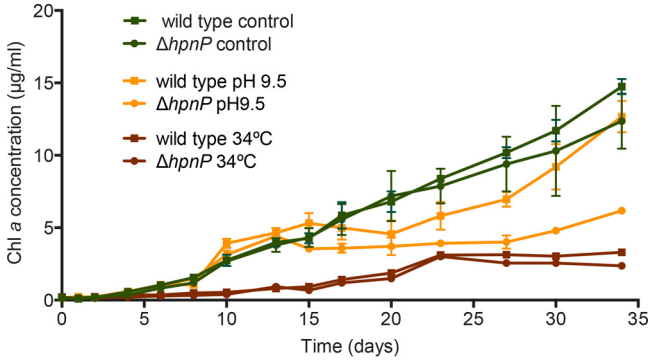

FIG 5 Growth curves of *N. punctiforme* wild-type and Δ*hpnP* mutant cultures grown under control (pH 7.8, 25°C), heat stress (34°C), and high pH stress (pH 9.5) conditions, based on chl *a* concentration. Error bars represent standard error (SE) from the mean of the results from three independent cultures.

Downloaded from http://aem.asm.org/ on June 7, 2018 by guest

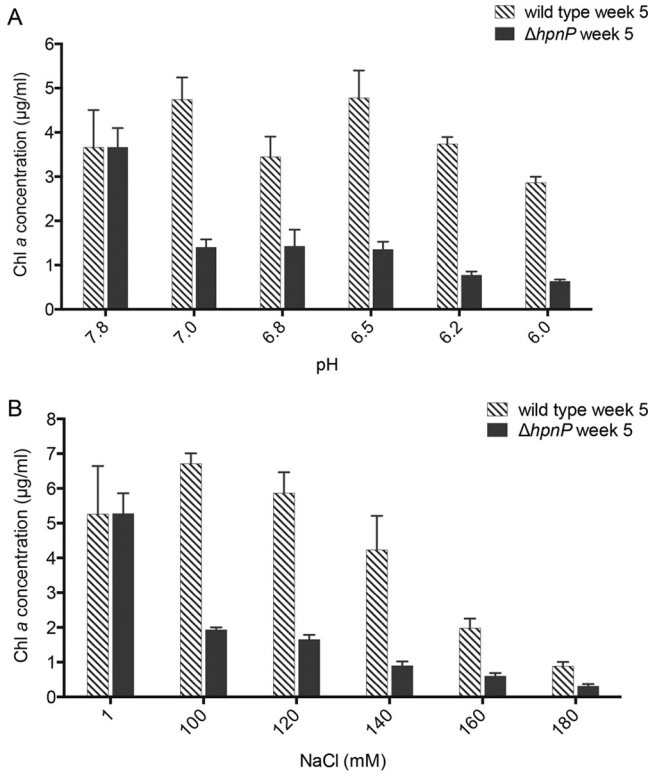

FIG 6 Density of *N. punctiforme* wild-type and Δ*hpnP* mutant cultures grown at a range of pH levels from 7.8 to 6.0 (A) or a range of NaCl concentrations from 1.1 mM to 180 mM (B) after 5 weeks. Measurements are relative to the density of cultures grown under control conditions (pH 7.8, 1.1 mM NaCl), based on chl *a* concentration. Error bars represent SE from the mean of the results from of three to four independent cultures. Culture densities at weeks 3 and 4 are shown in Fig. S2.

of the Δ*hpnP* mutant culture remained higher than those of the wild-type culture over this period.

A 3-(4,5-dimethylthiazol-2-yl)-2,5-diphenyltetrazolium bromide (MTT) assay was performed on *N. punctiforme* wild-type and Δ*hpnP* mutant cells that had been growing at pH levels from 6.0 to 7.8 for 4 weeks. The values were significantly higher for the mutant cells across all pH values from 6.0 to 7.0 (Fig. S4).

Δ*hpnP* mutant response to osmotic stress. *N. punctiforme* ATCC 29133S wild-type and Δ*hpnP* mutant cultures were subjected to a variety of different concentrations of NaCl in two different experimental designs. There was a significant difference in culture density between the wild-type and Δ*hpnP* mutant strains grown in concentrations of NaCl of 100 mM, 120 mM, 140 mM, 160 mM, and 180 mM for 5 weeks (Fig. 6B).

F_v/F_m was measured for control cultures and cultures grown at 100 mM NaCl over the course of 5 weeks. The F_v/F_m values of both NaCl-treated cultures were consistently higher than those of the control cultures, and the F_v/F_m values of the Δ*hpnP* mutant cells grown in 100 mM NaCl were significantly higher than those of the wild-type cells grown under the same conditions (Fig. S3C).

An MTT assay was performed on *N. punctiforme* wild-type and Δ*hpnP* mutant cells that had been growing at concentrations of NaCl from 1.1 mM to 180 mM for 4 weeks. Absorbance values were significantly higher for the mutant cells across all NaCl concentrations from 120 mM to 180 mM (Fig. S4).

DISCUSSION

Hopanoid production in the Δ*hpnP* mutant. It has previously been shown that in *Nostoc* sp. PCC 6720, 2-MeBHPs are produced in far greater abundance than their nonmethylated analogs (41). The results presented here were consistent with this. In the Δ*hpnP* mutant cells, the abundance of nonmethylated pentols increased by 1 to 2

Downloaded from http://aem.asm.org/ on June 7, 2018 by guest

orders of magnitude, resulting in the combined level of hopanoids being similar for the wild-type and Δ*hpnP* mutant cells. The increased production of BHpentol-1 and BHpentol-2 in the Δ*hpnP* mutant is likely a response to the inability to produce methylated hopanoids.

The lack of 2-MeBHPs in the Δ*hpnP* mutant cultures did not impede the cells' ability to form akinetes, which indicates these lipids are not essential for the formation of resting cells under normal conditions. However, as akinetes can survive extreme conditions (47, 48) that were not tested here, it may be that 2-MeBHP is more important for akinete survival against external stresses than for their formation; however, this is beyond the scope of the current study.

The present examination of akinete-dominated cultures of wild-type and Δ*hpnP* mutant cells was in accordance with the results of Doughty et al. (34), who found a large increase in the amount of 2-methylhopanoids, especially 2-MeBHtetrol, in akinete outer membranes of *N. punctiforme* compared to other cell membrane types. In the present study, no change in the relative abundances of 2-MeBHPs/BHPs was detected between vegetative cell and akinete-dominated cultures (Fig. 2). In comparing the quantitative aspects of the data, however, it is important to note that Doughty et al. (34) used GC-MS and conducted semiquantitative analyses of the lipid contents of isolated membrane fractions, as opposed to the data reported here, which are based on LC-MS and are for whole cells. More significantly, the bulk of BHP in this strain of *Nostoc punctiforme* is in the form of the two BHpentols and their methylated counterparts. These have longer retention times than BHtetrol and are likely less thermally stable. Thus, it is probable that a significant amount decomposed during the GC-MS analyses reported by Doughty et al. (34), as evidenced by the presence of a single BHpentol GC peak, thereby rendering the quantification less reliable in that earlier study. In this work, we also improved the quantitative rigor by employing an internal standard PD and authentic standards of BHtetrol and 2-MeBHtetrol (10) to determine the relative atmospheric pressure chemical ionization (APCI) response factors for these compounds, which were slightly but measurably different.

Response of Δ*hpnP* mutant to physiological stress. Cyanobacteria flourish in a variety of environments where factors, such as temperature, pH, and salt concentrations, are considered outside the optimal range for most bacteria. Cyanobacterial cells consequently have developed adaptations in order to protect themselves against these conditions. The culture conditions used here simulate those found in many extreme environments where cyanobacteria thrive, such as desert soil crusts, hot springs, hypersaline pools, and Antarctic melt water pools.

The Δ*hpnP* mutant was less resistant to pH and osmotic stress than the wild type. The role of 2-MeBHPs in stress tolerance against pH and osmotic stress is consistent with the findings of Kulkarni et al. (18) in *Rhodopseudomonas*, except that they found a regulatory effect on *hpnP* only in the presence of nonionic osmolytes.

The influence of hopanoids on the tolerance of temperature stresses has been investigated in *Rhodopseudomonas* (18) and *Nostoc punctiforme* (42). Our findings were in agreement with those of these two previous studies, as there were no significant differences between the growth rates or the PSII efficiency of wild-type and Δ*hpnP* mutant strains under elevated temperature. Studies of microbial mats from Antarctic melt water ponds (49) and Arctic soils (50) suggest that hopanoids may play a role in cryoprotection. We investigated this by subjecting the wild-type and Δ*hpnP* mutant strains to freezing in the absence of an exogenous cryoprotectant. The survival of wild-type cultures was greater than that of the Δ*hpnP* mutant, indicating that the absence of 2-MeBHPs decreases the tolerance of cells to freezing; however, this should be investigated more thoroughly at various temperatures and time scales.

F_v/F_m values reflect the efficiency of PSII, while MTT absorbance readings reflect the activities of NAD(P)H-dependent cellular oxidoreductases. Under control culture conditions, no differences in growth rate or F_v/F_m values were observed between the wild-type and Δ*hpnP* mutant cultures. However, when differences (albeit not statisti-

Downloaded from http://aem.asm.org/ on June 7, 2018 by guest

cally significant) in the growth rates between the two strains became apparent, these were reflected in differing F_v/F_m values and oxidoreductase activity (MTT assays). F_v/F_m values for the slower-growing Δ*hpnP* mutant cultures were higher than those for the wild-type cultures. From the MTT assays, the absorbance readings were higher for Δ*hpnP* mutant cells under salt and pH stress conditions than for wild-type cells under the same stress conditions. Taken together, the fact that values were consistently higher for Δ*hpnP* mutant cells than for wild-type cells under stress indicates an increased metabolic rate in the mutant strain, possibly as a compensatory stress response to reduced protection by hopanoids. This likely resulted in an increase in other protective strategies that require energy to maintain homeostasis rather than for growth. In addition, our finding of differences in the emission signals from the photosynthetic pigments in Δ*hpnP* mutant cultures, with substantial increases in phycoerythrin emissions in mutant akinete-dominated cultures compared to wild-type akinetes (and both vegetative cultures), may similarly be related to compensatory strategies in cells lacking hopanoids.

The presence of 2-MeBHPs does not appear to be necessary for *N. punctiforme* cell function under standard laboratory growth conditions. 2-MeBHPs do, however, appear to aid cyanobacterial cells to resist a variety of stress conditions, including pH and osmotic stress. Similar observations have been made in hopanoid mutants of *Burkholderia cenocepacia* (51) and *Rhodopseudomonas palustris* (19) that were attributed to a decrease in outer membrane integrity. While Doughty et al. (34) found that 2-MeBHPs were highest in akinetes, they are also present in vegetative cells, being localized between the cells of the filament (6). We observed that cells within Δ*hpnP* mutant filaments were not as closely packed (Fig. 3), with this decreased filament integrity at the cell-cell junction potentially increasing the sensitivity of the Δ*hpnP* mutant to stressors. Contrary to our original hypothesis, 2-MeBHPs were not necessary for *N. punctiforme* cells to form akinetes under phosphate-limiting and low-light conditions. Akinete outer membrane integrity is not impaired by the absence of 2-MeHPNs; however, the total absence of hopanoids (Δ*shc* mutant) results in a substantial decrease in akinete resilience, as determined by lysozyme treatment (42). However, the resistance of akinetes lacking 2-MeBHPs to other stresses has yet to be tested.

Conclusions. Given the importance of 2-MeBHPs in the adaptation to environmental stressors, such as pH, and their dominance in the resting cell type, the presence of 2-MeBHPs in geological sediment samples is indicative of periods of climate disturbances necessitating adaptation or senescence. As *hpnP* diversity was quite high in the desert environments sampled, testing of the resistance of the *N. punctiforme* Δ*hpnP* mutant to UV radiation and desiccation under conditions similar to those experienced by desert biological soil crust communities would be quite relevant (52). The preliminary evidence for a role for 2-MeBHPs in *N. punctiforme* in protection against freezing/thawing stress found here should be followed up with trials over different temperatures, cycles, and durations. Unfortunately, we cannot distinguish between the effects of smaller amounts of BHPs versus the loss of 2-MeBHP; however, complementary experiments utilizing a hopanoid-null mutant may further clarify their role. Overall, the *Nostoc punctiforme* Δ*hpnP* mutant created here provides a useful tool for investigating the role of 2-methylhopanoids in cyanobacteria.

MATERIALS AND METHODS

Knockout plasmid construction. The *hpnP* gene, along with flanking regions of at least 1 kb, was amplified from the genome of *Nostoc punctiforme* ATCC 29133S (UCD 153; a spontaneous ATCC 29133 derivate that grows more rapidly and homogenously in liquid, producing slow hormogonia [46]). The primers used for amplification (Table 1) incorporated XhoI restriction sites into the ends of the amplified product. This PCR product was ligated into the pGEM-T Easy (Promega) plasmid using the incorporated XhoI restriction sites. A central portion of the cloned *N. punctiforme hpnP* gene, consisting of 1,113 bp, was removed by digestion with the restriction enzymes MscI and AleI (New England BioLabs [NEB]).

The omega fragment containing the neomycin resistance gene (*npt*) and associated *psbA* promoter (PpsbA) of plasmid pSCR9 (53) was isolated by SmaI (NEB) restriction digestion. The recovered PpsbA-*npt* cassette from pSCR9 was ligated into the cleaved *hpnP* gene in the pGEM-T plasmid and transformed into

Downloaded from http://aem.asm.org/ on June 7, 2018 by guest

TABLE 1 Primers used for knockout mutant construction

Primer name	Sequence 5′ to 3′	Function
hpnP_NKOF	CTCGAGGGTGCAAGAGTCCTAATGGCGGG	Amplify *hpnP* and flanking regions from *N. punctiforme* ATCC 29133S genome and introduce XhoI restriction site for cloning into plasmid
hpnP_NKOR	CTCGAGAGTACAGTCTTGGCTTCACTGCCA	Amplify *hpnP* and flanking regions from *N. punctiforme* ATCC 29133S genome and introduce XhoI restriction site for cloning into plasmid
hpnP_IF	TAATCAAATGATGCCCCACA	Confirm removal of middle of *hpnP* gene in plasmid
hpnP_IR	ATTAATGAGCTTGCCCATCG	Confirm removal of middle of *hpnP* gene in plasmid
NptIntF	TTGGTGATCTCGCCTTTCACCTA	Confirm presence of neomycin resistance gene in plasmid
NptIntR	GGATGATCTGGACGAAGAGCATC	Confirm presence of neomycin resistance gene in plasmid
271F1	TGGAGTGAATACCACGACGA	Check sequence of knockout cassette in plasmid
271R1	TTGCCGGGAAGCTAGAGTAA	Check sequence of knockout cassette in plasmid
HNKO_seqF	GGCTTGACACAGGAATGGCGGTGG	Sequence *hpnP* and surrounding region from *N. punctiforme* Δ*hpnP* mutant genome
HNKO_seqR	GGCTGGTTAGCGCATATTGGCGTGG	Sequence *hpnP* and surrounding region from *N. punctiforme* Δ*hpnP* mutant genome
HNKO_seqF2	TGCCAGGAGCAAACCAGCAAC	Sequence *hpnP* and surrounding region from *N. punctiforme* Δ*hpnP* mutant genome
HNKO_seqR2	CGCTACTCGTTGTGTAATTCCGGT	Sequence *hpnP* and surrounding region from *N. punctiforme* Δ*hpnP* mutant genome
NRT_hpnPF1	TCGGGTTAGATACAGATACACCA	Confirm absence of middle of *hpnP* gene from *N. punctiforme* Δ*hpnP* mutant genome
NRT_hpnPF2	GGCATGGAAGTAGTATCAGGAAT	Confirm absence of middle of *hpnP* gene from *N. punctiforme* Δ*hpnP* mutant genome
NRT_hpnPR1	CCATAACGGAGTTCTAGGCAAA	Confirm absence of middle of *hpnP* gene from *N. punctiforme* Δ*hpnP* mutant genome
NRT_hpnPR2	GTTCTAGGCAAAGCATGAAGTAG	Confirm absence of middle of hpnP gene from *N. punctiforme* Δ*hpnP* mutant genome

competent *Escherichia coli* NEB 5-alpha cells (NEB). Colony PCR was used to screen for inserts containing the PpsbA-*npt* cassette, using the primers hpnP_IF and hpnP_IR (Table 1).

The *N. punctiforme hpnP* gene and flanking regions, with the inserted PpsbA-*npt* cassette, were removed from pGEM-T by digestion with the restriction enzyme XhoI (NEB). The plasmid pRL271 (54), a conjugative cyanobacterial suicide vector carrying a counterselective *sacB* gene for selection of double crossovers, was also digested with XhoI, and the resistance cassette was inserted. These plasmids were used to transform competent *E. coli* NEB 5-alpha (NEB) cells.

To confirm the sucrose sensitivity conferred by the *Bacillus subtilis* levansucrase *sacB* gene present in the pRL271 plasmid, *E. coli* colonies were grown in LB medium with 5% sucrose and 34 μg/ml chloramphenicol and compared to controls grown without sucrose.

Purified pRL271 containing the knockout cassette (referred to as HNKO) was used to transform *E. coli* TOP10 competent cells (Invitrogen).

Measurement of *N. punctiforme* culture density. The chlorophyll *a* (chl *a*) concentration was used to determine culture density. Duplicate aliquots of 500 μl or 1,000 μl were removed, and cells were collected by centrifugation. The supernatant was removed, and cells were resuspended in 90% methanol. Cells were lysed using a FastPrep FP120 cell disrupter (MP Biomedicals) instrument at speed of 6.0 for 40 s and then left to extract for at least 5 min in the dark. Aliquots were then centrifuged again, and the absorbance of the supernatant at 665 nm was measured. The concentration of chl *a* was calculated by multiplying the average A_{665} reading by 12.7 to obtain the micrograms of chl *a* per milliliter (55).

Triparental conjugation. The HNKO plasmid was introduced into *Nostoc punctiforme* 29133S by triparental conjugation, as previously described (56) (http://microbiology.ucdavis.edu/meeks/xpro3.htm), with minor modifications, as follows. Briefly, *E. coli* TOP10 harboring HNKO plasmid (donor strain) and *E. coli* JCM113 (helper strain; *E. coli* HB101 carrying both pRK2013 and pRL528 plasmids for mobilization and methylation, respectively) were grown in LB medium containing both chloramphenicol and kanamycin, at 30°C, until cultures reached an OD_{600} of about 0.7. Cells were washed, concentrated to an OD_{600} of 9 to 10, gently mixed, and incubated at room temperature for ~1 h.

Nostoc punctiforme ATCC 29133S cells from a dense 500-ml culture were harvested by centrifugation and resuspended in 30 ml of fresh Allen & Arnon medium diluted 4-fold (A&A/4). Cultures were disrupted with a Branson digital sonicator in order to fragment filaments to a length of 1 to 4 cells. Cells were harvested, resuspended in A&A/4 medium containing 5 mM morpholinepropanesulfonic acid (MOPS) (pH 7.8) and 2.5 mM NH_4Cl, and placed in low light (~5 to 10 microeinsteins · m^2 · s^{-1}) to recover for at least 4 h, prior to concentration of the cells to a chl *a* concentration of 100 μg of chl *a*/ml.

Sterile conjugation filters (HATF08250, 0.45 μm, 82 mm; Millipore) were placed on 1% A&A agar plates containing 5 mM MOPS (pH 7.8), 2.5 mM NH_4Cl, and 0.5% LB. Equal amounts (500 μl) of *N. punctiforme* culture and *E. coli* mixture were combined and briefly centrifuged. The supernatant was removed, and the remaining culture was spread onto a conjugation filter. Plates were placed in low light (~5 to 10 microeinsteins · m^2 · s^{-1}) at 25°C overnight. All conjugation filters were then transferred to plain 1% A&A agar plates and incubated for a further 4 days.

Downloaded from http://aem.asm.org/ on June 7, 2018 by guest

Growth and selection of Δ*hpnP* mutants. Conjugation filters were transferred to 1% A&A plates containing 25 μg/ml neomycin and placed in high light (~25 to 30 microeinsteins · m^2 · s^{-1}) at 25°C. *N. punctiforme* colonies that grew on the neomycin selection plates were transferred to 0.5 ml of A&A/4 medium with 25 μg/ml neomycin and incubated for 2 weeks. At this point, to induce resolution and exclusion of the pRL271 plasmid backbone, the cultures were transferred to 4 ml of A&A/4 medium without neomycin and incubated for 2 weeks. Cells were recovered by centrifugation, resuspended in 0.5 ml of medium, and vortexed. Cells were spread onto 1% A&A agar plates containing 5 mM MOPS, 25 μg/ml neomycin, and 5% (wt/vol) sucrose to select against cells retaining the pRL271 plasmid backbone, which carries the *sacB* gene. Sucrose-resistant colonies were screened by PCR to confirm resolution by double crossover (Fig. S1). The Δ*hpnP* mutant strain was maintained in A&A/4 medium with 25 μg/ml neomycin.

Confirmation of 2-methylhopanoid absence/gene inactivation. Detection and quantification of hopanoids by high-performance liquid chromatography-mass spectrometry (HPLC-MS) was used to confirm the absence of 2-MeBHP production and assess the production of other BHP compounds in cultures. A fraction of each total lipid extract (TLE) was acetylated with pyridine-acetic anhydride (1:1 [vol/vol]) at 70°C for 1 h and left at room temperature overnight. The acetylated TLEs were analyzed by LC-MS. The LC-MS system comprises a 1200 series HPLC (Agilent Technologies, Santa Clara, CA, USA) equipped with an autosampler and a binary pump linked to a quadrupole time of flight (Q-TOF) 6520 mass spectrometer (Agilent Technologies) via an atmospheric pressure chemical ionization (APCI) interface (Agilent Technologies) operated in positive-ion mode. The analytical procedure was adapted from a study by Talbot et al. (57). A Poroshell 120 EC-C_{18} column (2.1 by 150 mm, 2.7 μm; Agilent Technologies) was chosen to provide fast and high-resolution separations at lower pressures. The APCI parameters were as follows: gas temperature, 325°C; vaporizer temperature, 350°C; drying gas (N_2) flow, 6 liters/min; nebulizer (N_2) flow, 30 liters/min; capillary voltage, 1,200 V; corona needle, 4 μA; and fragmentor, 150 V.

Hopanoids were identified on the basis of accurate mass measurements of their protonated molecular ions, of fragmentation patterns in tandem MS (MS-MS) mode, and by comparison (Fig. 1) of relative retention times (58–60). Quantification was accomplished using an external standard, 5β-pregnane-3α,12α-diol-20-one diacetate (PD), chosen because of its structural similarity to hopanoids and because its retention time does not overlap BHP retention times. However, considerable variability exists in the ionization efficiencies of all hopanoid structures, especially compared to PD (10). Therefore, the relative response factors for BHtetrol and 2-MeBHtetrol were determined using authentic standards and applied to the quantification of all BHP compounds in this study. The relative responses of all BHP, relative to PD, were previously observed to be linear over four orders of magnitude (1). Without equivalent standards for BHpentol and 2-MeBHpentol, however, our quantification can be considered only approximate for those particular compounds. Since this study focuses on the relative abundance of BHPs, precise quantification for all compounds is not required.

Akinete formation and microscopy. To induce akinete differentiation, cells were transferred to A&A medium without phosphate (61) and placed in very low light (~1 to 2 microeinsteins · m^2 · s^{-1}). Cells were maintained under these conditions for several weeks. Akinete formation was checked periodically by light microscopy. Sample preparation and electron microscope imaging was performed using an FEI Nova NanoSEM 230 FE-SEM instrument. Cellular morphology of live *N. punctiforme* cultures was examined by Leica TCS SP5 confocal inverted microscope (Leica Microsystems, Heidelberg, Germany). Imaging was performed at excitation by a 488-nm line of argon laser and by 633 nm line of HeNe laser, with emissions at 520 to 620 nm captured in photomultiplier tube (PMT) 1 and emissions at 638 to 720 nm captured in PMT 2, respectively. Fluorescence emissions from photosynthetic pigments in vegetative and akinete cells (n = 3 to 4), mainly phycobiliproteins and chlorophyll *a* (chl *a*), were microspectrally characterized using the λ scan mode of Leica SP5 at excitation by 488 nm by sequentially imaging a series of images from 500 to 750 nm, each acquired at 10-nm emission detection bandwidth, with 5-nm steps. Spectral data from defined regions of interests (ROIs) inside cells obtained from Leica LAS software were imported into an Excel spreadsheet and plotted.

Stress treatments. *Nostoc punctiforme* ATCC 29133S wild-type and Δ*hpnP* mutant cultures were subjected to a variety of stress conditions. Cells were grown in A&A/4 medium (without neomycin) at 25°C on a shaking platform under cool white fluorescent lights (~20 microeinsteins · m^2 · s^{-1}) until they reached mid-log phase and then were transferred to the stress treatments. Two different experimental designs for growing cells under stress conditions were used, covering a range of temperatures, pH levels, and salt concentrations. The standard growth conditions used for control cultures in all experiments were 25°C, 1.1 mM NaCl, and pH 7.8.

First, cultures were subjected to heat stress (34°C), osmotic stress (100 mM NaCl), and pH stress (6.0 and 9.5). The media for control, salt, and heat stress treatments were buffered to pH 7.8 with 10 mM HEPES. The medium for the pH 9.5 treatment was buffered with 10 mM sodium carbonate-sodium bicarbonate, and the medium for the pH 6.0 treatment was buffered with 10 mM morpholineethanesulfonic acid (MES). Three biological replicates were maintained for each treatment under continuous light on a shaking platform. At the beginning of the trial, 130 ml of each type of medium was inoculated with cells at an initial density of approximately 0.1 μg of chl *a*/ml. Growth was measured over the course of several weeks by chl *a* extraction, as described above. The maximum quantum yield of photosystem II (PSII) (F_v/F_m) of each culture was also measured at various times over the course of the trial, as described below.

Second, a range of pH levels and NaCl concentrations were evaluated concurrently. The range of pH levels was from 4.8 to 10.0, and the range of NaCl concentrations was 100 to 180 mM. Four biological

Downloaded from http://aem.asm.org/ on June 7, 2018 by guest

replicates were maintained for each treatment under continuous light on a shaking platform. Cultures were grown in a 24-well plate, where 2 ml of medium in each well was inoculated with cells at an initial density of approximately 0.6 μg of chl *a*/ml. Media for cultures grown at pH levels from 6.0 to 6.5 were buffered with 10 mM MES, media for cultures grown at pH levels from 6.8 to 8.2 were buffered with 10 mM HEPES, and media for cultures grown at pH levels from 8.5 to 9.0 were buffered with 10 mM Tris. Growth was measured over the course of several weeks by chl *a*, and MTT [3-(4,5-dimethylthiazol-2-yl)-2,5-diphenyltetrazolium bromide] assays were performed as described below.

Cells were also subjected to stress caused by freezing. Cultures were concentrated by centrifugation to approximately 12 μg of chl *a*/ml, and then 1-ml aliquots were vortexed to homogenize cultures. These 1-ml aliquots were placed in a freezer at −20°C in two sets of biological triplicates. One set was thawed and refrozen twice over 1 week, and the second set was thawed and refrozen three times over 2 weeks. After final removal from the freezer, thawed cells were used to inoculate 50 ml of A&A/4 medium and left to recover under control conditions. Growth was measured over the course of several weeks by chl *a* extraction.

PAM fluorometry. A portable pulse amplitude modulation (PAM) fluorometer 2500 (Walz) was used to measure F_v/F_m. F_v/F_m is an indicator of PSII efficiency, which can in turn be used as an indicator of overall cell health. Aliquots of 1 ml were removed from cultures, adapted to the dark for a minimum of 10 min, and then placed under a weak red measuring light. Cells were exposed to a strong red saturation pulse of 100 ms in duration to measure the maximum (dark-adapted) yield of PSII (F_v/F_m). Slow kinetics curves were determined for cells from each treatment by applying red actinic light for 250 s, with a saturation pulse every 20 s.

MTT assays. The MTT assay was used to assess cell proliferation based on the NAD(P)H-dependent oxidoreductase enzyme activity of cells. Cell densities were standardized to the lowest density present according to chl *a* measurements. Cells were resuspended in 100 μl of medium in a 96-well plate, using four biological replicates for each treatment. A 20-μl solution of 5 mg/ml thiazolyl blue tetrazolium blue (MTT; Sigma-Aldrich) was added, and samples were incubated at 37°C for 2 h. Plates were centrifuged, medium was removed from the wells, and 200 μl of acidic isopropanol (0.04 M HCl) was added to each well and mixed. Absorbance was measured at 570 nm, with higher absorbance readings corresponding to a higher level of metabolic function.

Statistical analysis. Slopes of the exponential-phase growth curves for cultures treated by heat stress, pH 6.0, pH 9.5, 100 mM NaCl, and freezing were calculated in Prism version 6.0, and one-way analysis of variance (ANOVA) was performed to compare slopes.

For cell densities of cultures grown in a range of pH levels and NaCl concentrations, values were adjusted to account for differences between cultures of wild-type and Δ*hpnP* mutant cells under control conditions. Assuming exponential growth, the growth rates of the treatment cultures were normalized to average control culture growth rates at each time point using the formula $\text{density}A_x \times (\text{density}B_{\text{control\_average}}/\text{density}A_{\text{control\_average}})$, where A is the slower-growing culture under optimal conditions and B is the faster-growing culture under optimal conditions. The densities of the cultures in each treatment at each time point were compared separately by one-way ANOVA.

For MTT assays, values were adjusted to account for differences between cultures of wild-type and Δ*hpnP* mutant cells under control conditions. Assuming a linear relationship between NAD(P)H-dependent enzyme activity and the A_{570} values observed, the values for the treatment cultures were normalized to the average control culture values at each time point using the formula $\text{density}A_x + (\text{density}B_{\text{control\_average}} - \text{density}A_{\text{control\_average}})$. A and B are defined as described above. The absorbance readings of assays from each treatment at each time point were compared separately by one-way ANOVA.

SUPPLEMENTAL MATERIAL

Supplemental material for this article may be found at https://doi.org/10.1128/AEM.00777-17.

SUPPLEMENTAL FILE 1, PDF file, 0.8 MB.

ACKNOWLEDGMENTS

We acknowledge the services of the University of New South Wales Electron Microscopy Unit and the Ramaciotti Centre for Genomics. We thank C. H. Wu and D. K. Newman for the provision of authentic standards of BHtetrol and 2-MeBHtetrol, and J. C. Meeks for provision of the *N. punctiforme* 29133S and *E. coli* JCM113 strains.

Work undertaken at UNSW was supported by The Australian Research Council. Work undertaken at MIT was supported by an award (NNA13AA90A) from the NASA Astrobiology Institute.

REFERENCES

1. Sáenz JP, Waterbury JB, Eglinton TI, Summons RE. 2012. Hopanoids in marine cyanobacteria: probing their phylogenetic distribution and biological role. Geobiology 10:311–319. https://doi.org/10.1111/j.1472-4669.2012.00318.x.

Downloaded from http://aem.asm.org/ on June 7, 2018 by guest

2. Ourisson G, Albrecht P. 1992. Hopanoids. 1. Geohopanoids: the most abundant natural products on Earth? Acc Chem Res 25:398–402. https://doi.org/10.1021/ar00021a003.
3. Kannenberg EL, Perzl M, Müller P, Härtner T, Poralla K. 1996. Hopanoid lipids in *Bradyrhizobium* and other plant-associated bacteria and cloning of the *Bradyrhizobium japonicum* squalene-hopene cyclase gene. Plant Soil 186:107–112. https://doi.org/10.1007/BF00035063.
4. Kannenberg EL, Poralla K. 1999. Hopanoid biosynthesis and function in bacteria. Naturwissenschaften 86:168–176. https://doi.org/10.1007/s001140050592.
5. Doughty DM, Coleman ML, Hunter RC, Sessions AL, Summons RE, Newman DK. 2011. The RND-family transporter, HpnN, is required for hopanoid localization to the outer membrane of *Rhodopseudomonas palustris* TIE-1. Proc Natl Acad Sci U S A 108:E1045–E1051. https://doi.org/10.1073/pnas.1104209108.
6. Doughty DM, Dieterle M, Sessions AL, Fischer WW, Newman DK. 2014. Probing the subcellular localization of hopanoid lipids in bacteria using NanoSIMS. PLoS One 9:e84455. https://doi.org/10.1371/journal.pone.0084455.
7. Jürgens UJ, Simonin P, Rohmer M. 1992. Localization and distribution of hopanoids in membrane systems of the cyanobacterium *Synechocystis* PCC 6714. FEMS Microbiol Lett 71:285–288. https://doi.org/10.1016/0378-1097(92)90723-2.
8. Simonin P, Jürgens UJ, Rohmer M. 1996. Bacterial triterpenoids of the hopane series from the prochlorophyte *Prochlorothrix hollandica* and their intracellular localization. Eur J Biochem 241:865–871. https://doi.org/10.1111/j.1432-1033.1996.00865.x.
9. Poralla K, Kannenberg E, Blume A. 1980. A glycolipid containing hopane isolated from the acidophilic, thermophilic *Bacillus acidocaldarius*, has a cholesterol-like function in membranes. FEBS Lett 113:107–110. https://doi.org/10.1016/0014-5793(80)80506-0.
10. Wu C-H, Bialecka-Fornal M, Newman DK. 2015. Methylation at the C-2 position of hopanoids increases rigidity in native bacterial membranes. eLife 4:e05663. https://doi.org/10.7554/eLife.05663.
11. Silipo A, Vitiello G, Gully D, Sturiale L, Chaintreuil C, Fardoux J, Gargani D, Lee H-I, Kulkarni G, Busset N, Marchetti R, Palmigiano A, Moll H, Engel R, Lanzetta R, Paduano L, Parrilli M, Chang W-S, Holst O, Newman DK, Garozzo D, D'Errico G, Giraud E, Molinaro A. 2014. Covalently linked hopanoid-lipid A improves outer-membrane resistance of a *Bradyrhizobium* symbiont of legumes. Nat Commun 5:5106. https://doi.org/10.1038/ncomms6106.
12. Komaniecka I, Choma A, Mazur A, Duda KA, Lindner B, Schwudke D, Holst O. 2014. Occurrence of an unusual hopanoid-containing lipid A among lipopolysaccharides from *Bradyrhizobium* species. J Biol Chem 289:35644–35655. https://doi.org/10.1074/jbc.M114.614529.
13. Sáenz JP, Grosser D, Bradley AS, Lagny TJ, Lavrynenko O, Broda M, Simons K. 2015. Hopanoids as functional analogues of cholesterol in bacterial membranes. Proc Natl Acad Sci U S A 112:11971–11976. https://doi.org/10.1073/pnas.1515607112.
14. Caron B, Mark AE, Poger D. 2014. Some like it hot: the effect of sterols and hopanoids on lipid ordering at high temperature. J Phys Chem Lett 5:3953–3957. https://doi.org/10.1021/jz5020778.
15. Joyeux C, Fouchard S, Llopiz P, Neunlist S. 2004. Influence of the temperature and the growth phase on the hopanoids and fatty acids content of *Frateuria aurantia* (DSMZ 6220). FEMS Microbiol Ecol 47:371–379. https://doi.org/10.1016/S0168-6496(03)00302-7.
16. Poralla K, Htrtner T, Kannenberg E. 1984. Effect of temperature and pH on the hopanoid content of *Bacillus acidocaldarius*. FEMS Microbiol Lett 23:253–256. https://doi.org/10.1111/j.1574-6968.1984.tb01073.x.
17. Schmidt A, Bringer-Meyer S, Poralla K, Sahm H. 1986. Effect of alcohols and temperature on the hopanoid content of *Zymomonas mobilis*. Appl Microbiol Biotechnol 25:32–36. https://doi.org/10.1007/BF00252509.
18. Kulkarni G, Wu C-H, Newman DK. 2013. The general stress response factor EcfG regulates expression of the C-2 hopanoid methylase HpnP in *Rhodopseudomonas palustris* TIE-1. J Bacteriol 195:2490–2498. https://doi.org/10.1128/JB.00186-13.
19. Welander PV, Hunter RC, Zhang L, Sessions AL, Summons RE, Newman DK. 2009. Hopanoids play a role in membrane integrity and pH homeostasis in *Rhodopseudomonas palustris* TIE-1. J Bacteriol 191:6145–6156. https://doi.org/10.1128/JB.00460-09.
20. Poralla K, Muth G, Härtner T. 2000. Hopanoids are formed during transition from substrate to aerial hyphae in *Streptomyces coelicolor* A3(2). FEMS Microbiol Lett 189:93–95. https://doi.org/10.1111/j.1574-6968.2000.tb09212.x.
21. Jahnke LL, Embaye T, Hope J, Turk KA, Van Zullen M, Des Marais DJ, Farmer JD, Summons RE. 2004. Lipid biomarker and carbon isotopic signatures for stromatolite-forming, microbial mat communities and *Phormidium* cultures from Yellowstone National Park. Geobiology 2:31–47. https://doi.org/10.1111/j.1472-4677.2004.00021.x.
22. Summons RE, Jahnke LL, Hope JM, Logan GA. 1999. 2-Methylhopanoids as biomarkers for cyanobacterial oxygenic photosynthesis. Nature 400:554–557. https://doi.org/10.1038/23005.
23. Talbot HM, Summons RE, Jahnke LL, Cockell CS, Rohmer M, Farrimond P. 2008. Cyanobacterial bacteriohopanepolyol signatures from cultures and natural environmental settings. Org Geochem 39:232–263. https://doi.org/10.1016/j.orggeochem.2007.08.006.
24. Knoll AH, Summons RE, Waldbauer JR, Zumberge J. 2007. The geological succession of primary producers in the oceans, p 133–163. *In* Falkowski PG, Knoll AH (ed), Evolution of primary producers in the sea. Elsevier, Boston, MA.
25. Kuypers MMM, van Breugel Y, Schouten S, Erba E, Sinninghe Damsté JS. 2004. N_2-fixing cyanobacteria supplied nutrient N for Cretaceous oceanic anoxic events. Geology 32:853. https://doi.org/10.1130/G20458.1.
26. Bisseret P, Zundel M, Rohmer M. 1985. Prokaryotic triterpenoids. 2. 2β-methylhopanoids from *Methylobacterium organophilum* and *Nostoc muscorum*, a new series of prokaryotic triterpenoids. Eur J Biochem 150:29–34. https://doi.org/10.1111/j.1432-1033.1985.tb08982.x.
27. Bravo JM, Perzl M, Härtner T, Kannenberg EL, Rohmer M. 2001. Novel methylated triterpenoids of the gammacerane series from the nitrogen-fixing bacterium *Bradyrhizobium japonicum* USDA 110. Eur J Biochem 268:1323–1331. https://doi.org/10.1046/j.1432-1327.2001.01998.x.
28. Renoux JM, Rohmer M. 1985. Prokaryotic triterpenoids. New bacteriohopanetetrol cyclitol ethers from the methylotrophic bacterium *Methylobacterium organophilum*. Eur J Biochem 151:405–410. https://doi.org/10.1111/j.1432-1033.1985.tb09116.x.
29. Stampf P, Herrmann D, Bisseret P, Rohmer M. 1991. 2α-Methylhopanoids: First recognition in the bacterium *Methylobacterium organophilum* and obtention via sulphur induced isomerization of 2β-methylhopanoid. An account for their presence in sediments. Tetrahedron 47:7081–7990. https://doi.org/10.1016/s0040-4020(01)96162-9.
30. Vilcheze C, Llopiz P, Neunlist S, Poralla K, Rohmer M. 1994. Prokaryotic triterpenoids: new hopanoids from the nitrogen-fixing bacteria *Azotobacter vinelandii*, *Beijerinckia indica* and *Beijerinckia mobilis*. Microbiology 140:2749–2753. https://doi.org/10.1099/00221287-140-10-2749.
31. Rashby SE, Sessions AL, Summons RE, Newman DK. 2007. Biosynthesis of 2-methylbacteriohopanepolyols by an anoxygenic phototroph. Proc Natl Acad Sci U S A 104:15099–15104. https://doi.org/10.1073/pnas.0704912104.
32. Ricci JN, Michel AJ, Newman DK. 2015. Phylogenetic analysis of HpnP reveals the origin of 2-methylhopanoid production in Alphaproteobacteria. Geobiology 13:267–277. https://doi.org/10.1111/gbi.12129.
33. Ricci JN, Coleman ML, Welander PV, Sessions AL, Summons RE, Spear JR, Newman DK. 2014. Diverse capacity for 2-methylhopanoid production correlates with a specific ecological niche. ISME J 8:675–684. https://doi.org/10.1038/ismej.2013.191.
34. Doughty DM, Hunter RC, Summons RE, Newman DK. 2009. 2-Methylhopanoids are maximally produced in akinetes of *Nostoc punctiforme*: geobiological implications. Geobiology 7:524–532. https://doi.org/10.1111/j.1472-4669.2009.00217.x.
35. Rippka R, Deruelles J, Waterbury JB, Herdman M, Stanier RY. 1979. Generic assignments, strain histories and properties of pure cultures of cyanobacteria. Microbiology 111:1–61. https://doi.org/10.1099/00221287-111-1-1.
36. Meeks JC. 1998. Symbiosis between nitrogen-fixing cyanobacteria and plants. Bioscience 48:266–276. https://doi.org/10.2307/1313353.
37. Meeks JC, Campbell EL, Summers ML, Wong FC. 2002. Cellular differentiation in the cyanobacterium *Nostoc punctiforme*. Arch Microbiol 178:395–403. https://doi.org/10.1007/s00203-002-0476-5.
38. Meeks JC, Elhai J, Thiel T, Potts M, Larimer F, Lamerdin J, Predki P, Atlas R. 2001. An overview of the genome of *Nostoc punctiforme*, a multicellular, symbiotic cyanobacterium. Photosynth Res 70:85–106. https://doi.org/10.1023/A:1013840025518.
39. Welander PV, Coleman ML, Sessions AL, Summons RE, Newman DK. 2010. Identification of a methylase required for 2-methylhopanoid production and implications for the interpretation of sedimentary hopanes. Proc Natl Acad Sci U S A 107:8537–8542. https://doi.org/10.1073/pnas.0912949107.
40. Rohmer M, Bouviernave P, Ourisson G. 1984. Distribution of hopanoid

Downloaded from http://aem.asm.org/ on June 7, 2018 by guest

triterpenes in prokaryotes. J Gen Microbiol 130:1137–1150. https://doi.org/10.1099/00221287-130-5-1137.
41. Zhao N, Berova N, Nakanishi K. 1996. Structures of two bacteriohopanoids with acyclic pentol side-chains from the cyanobacterium *Nostoc* PCC 6720. Tetrahedron 52:2777–2788. https://doi.org/10.1016/0040-4020(96)00013-0.
42. Ricci JN, Morton R, Kulkarni G, Summers ML, Newman DK. 2016. Hopanoids play a role in stress tolerance and nutrient storage in the cyanobacterium *Nostoc punctiforme*. Geobiology 15:173–183. https://doi.org/10.1111/gbi.12204.
43. Sepúlveda J, Wendler J, Leider A, Kuss H-J, Summons RE, Hinrichs K-U. 2009. Molecular isotopic evidence of environmental and ecological changes across the Cenomanian–Turonian boundary in the Levant Platform of central Jordan. Org Geochem 40:553–568. https://doi.org/10.1016/j.orggeochem.2009.02.009.
44. Sepúlveda J, Wendler JE, Summons RE, Hinrichs K-U. 2009. Rapid resurgence of marine productivity after the Cretaceous-Paleogene mass extinction. Science 326:129–132. https://doi.org/10.1126/science.1176233.
45. French KL, Tosca NJ, Cao C, Summons RE. 2012. Diagenetic and detrital origin of moretane anomalies through the Permian–Triassic boundary. Geochim Cosmochim Acta 84:104–125. https://doi.org/10.1016/j.gca.2012.01.004.
46. Campbell EL, Summers ML, Christman H, Martin ME, Meeks JC. 2007. Global gene expression patterns of *Nostoc punctiforme* in steady-state dinitrogen-grown heterocyst-containing cultures and at single time points during the differentiation of akinetes and hormogonia. J Bacteriol 189:5247–5256. https://doi.org/10.1128/JB.00360-07.
47. Olsson-Francis K, de la Torre R, Towner MC, Cockell CS. 2009. Survival of akinetes (resting-state cells of cyanobacteria) in low earth orbit and simulated extraterrestrial conditions. Orig Life Evol Biosph 39:565–579. https://doi.org/10.1007/s11084-009-9167-4.
48. Yamamoto Y. 1975. Effect of desiccation on the germination of akinetes of *Anabaena cylindrica*. Plant Cell Physiol 16:749–752. https://doi.org/10.1093/oxfordjournals.pcp.a075195.
49. Jungblut AD, Allen MA, Burns BP, Neilan BA. 2009. Lipid biomarker analysis of cyanobacteria-dominated microbial mats in meltwater ponds on the McMurdo Ice Shelf, Antarctica. Org Geochem 40:258–269. https://doi.org/10.1016/j.orggeochem.2008.10.002.
50. Rethemeyer J, Schubotz F, Talbot HM, Cooke MP, Hinrichs K-U, Mollenhauer G. 2010. Distribution of polar membrane lipids in permafrost soils and sediments of a small high Arctic catchment. Org Geochem 41:1130–1145. https://doi.org/10.1016/j.orggeochem.2010.06.004.
51. Schmerk CL, Bernards MA, Valvano MA. 2011. Hopanoid production is required for low-pH tolerance, antimicrobial resistance, and motility in *Burkholderia cenocepacia*. J Bacteriol 193:6712–6723. https://doi.org/10.1128/JB.05979-11.
52. Rajeev L, da Rocha UN, Klitgord N, Luning EG, Fortney J, Axen SD, Shih PM, Bouskill NJ, Bowen BP, Kerfeld CA, Garcia-Pichel F, Brodie EL, Northen TR, Mukhopadhyay A. 2013. Dynamic cyanobacterial response to hydration and dehydration in a desert biological soil crust. ISME J 7:2178–2191. https://doi.org/10.1038/ismej.2013.83.
53. Cohen MF, Meeks JC. 1997. A hormogonium regulating locus, *hrmUA*, of the cyanobacterium *Nostoc punctiforme* strain ATCC 29133 and its response to an extract of a symbiotic plant partner *Anthoceros punctatus*. Mol Plant Microbe Interact 10:280–289. https://doi.org/10.1094/MPMI.1997.10.2.280.
54. Cai YP, Wolk CP. 1990. Use of a conditionally lethal gene in *Anabaena* sp. strain PCC 7120 to select for double recombinants and to entrap insertion sequences. J Bacteriol 172:3138–3145. https://doi.org/10.1128/jb.172.6.3138-3145.1990.
55. Meeks JC, Castenholz RW. 1971. Growth and photosynthesis in an extreme thermophile, *Synechococcus lividus* (Cyanophyta). Arch Mikrobiol 78:25–41. https://doi.org/10.1007/BF00409086.
56. Cohen MF, Wallis JG, Campbell EL, Meeks JC. 1994. Transposon mutagenesis of Nostoc sp. strain ATCC 29133, a filamentous cyanobacterium with multiple cellular differentiation alternatives. Microbiology 140:3233–3240. https://doi.org/10.1099/13500872-140-12-3233.
57. Talbot HM, Watson DF, Murrell JC, Carter JF, Farrimond P. 2001. Analysis of intact bacteriohopanepolyols from methanotrophic bacteria by reversed-phase high-performance liquid chromatography-atmospheric pressure chemical ionisation mass spectrometry. J Chromatogr A 921:175–185. https://doi.org/10.1016/S0021-9673(01)00871-8.
58. Talbot HM, Rohmer M, Farrimond P. 2007. Rapid structural elucidation of composite bacterial hopanoids by atmospheric pressure chemical ionisation liquid chromatography/ion trap mass spectrometry. Rapid Commun Mass Spectrom 21:880–892. https://doi.org/10.1002/rcm.2911.
59. Talbot HM, Summons R, Jahnke L, Farrimond P. 2003. Characteristic fragmentation of bacteriohopanepolyols during atmospheric pressure chemical ionisation liquid chromatography/ion trap mass spectrometry. Rapid Commun Mass Spectrom 17:2788–2796. https://doi.org/10.1002/rcm.1265.
60. Welander PV, Doughty DM, Wu CH, Mehay S, Summons RE, Newman DK. 2012. Identification and characterization of *Rhodopseudomonas palustris* TIE-1 hopanoid biosynthesis mutants. Geobiology 10:163–177. https://doi.org/10.1111/j.1472-4669.2011.00314.x.
61. Wong FCY, Meeks JC. 2002. Establishment of a functional symbiosis between the cyanobacterium *Nostoc punctiforme* and the bryophyte *Anthoceros punctatus* requires genes involved in nitrogen control and initiation of heterocyst differentiation. Microbiology 148:315–323. https://doi.org/10.1099/00221287-148-1-315.

Downloaded from http://aem.asm.org/ on June 7, 2018 by guest